Journal of Ceramic Processing Research. Vol. 17, No. 11, pp. 1143~1147 (2016)

J O U R N A L O F
Ceramic Processing Research

Microstructure and mechanical properties of spark plasma sintered alumina-based composites reinforced with WC

D. Ghahremani[a], I. Mobasherpour[b,*], M. Razavi[b], H. Eslami Shahed[b] and H. Rajaei[b]
[a]*Engineering department, Maybod Branch, Islamic Azad University, Maybod, Iran*
[b]*Ceramics Department, Materials and Energy Research Center, P.O. Box 31787-316, Karaj, Iran*

Alumina-based composites reinforced with WC were fabricated by powder processing techniques and consolidated by spark plasma sintering. Microstructure, strength, hardness and fracture toughness of the Al_2O_3-WC composites were studied. The Al_2O_3-WC composite containing 5-20 wt% WC reached over 95% theoretical density at 1650 °C and nearly full density at 1700 °C. The strength, Vickers hardness and fracture toughness of Al_2O_3-(10 wt. %)WC composite sintered at 1700 °C reached a maximum value of 463 MPa, 2208 HV, and 4.15 MPa.m$^{1/2}$ respectively.

Key words: Alumina, WC, Composite, Spark plasma sintering.

Introduction

Nowadays alumina reinforced with micro and nano-sized carbides, such as TiC, WC, AlTiC and ZrO_2 is categorized as a new class of hard materials with improved mechanical properties [1-4]. The reinforcement with the above carbides can also improve the wear properties of alumina matrices [5]. Although cutting machinery markets are still dominated by WC-Co tools, alumina-based composite materials are a good alternative to improve the cutting speed and lower the production cost [6].

As widely described in literature, sintering of oxide matrix composites reinforced by WC particles is a typical example of a sintering with "rigid inclusions [7-9]. In fact, during this process, diffusional mechanisms of densifications appear only in the oxide matrix. The presence of carbide particles makes the sintering driving forces much weaker. This effect becomes stronger for the higher volume contents of tungsten carbide particles. The high relative density demand for structural applications (> 97% of TD) can be satisfied using pressureless sintering method as long as WC content does not exceed 20 vol. %. Additionally, sintering temperature for pressureless sintering must be relatively high (1550 °C for zirconia and 1600 °C for alumina). Nevertheless, such a high sintering temperature is not recommended for sintered microstructures because of occurrence of the excessive grain growth [10, 11]. In comparison with conventional sintering methods, SPS is a process that is capable of sintering ceramic powders quickly to their full density at a relatively low temperature [12].

*Corresponding author:
Tel : +98(261)6204131-4
Fax: +98(261)6201888
E-mail: Iman.Mobasherpour@gmail.com, i_mobasherpour@merc.ac.ir

SPS or plasma pressure compaction is a technique for densifying any classes of materials, especially for the materials that are difficult to be sintered by conventional techniques. The presence of plasma in the SPS system is still unproven. Specific advantages of SPS over conventional sintering techniques are (1) faster heating rate, which avoids the mass transport mechanisms that do not contribute to densification (2) shorter dwell times, which retain finer microstructures and (3) DC pulse voltage that contributes to an enhanced mass transport through the electro-migration [13-19]. In this study, Al_2O_3-WC composites were prepared by SPS of WC and Al_2O_3 powder mixtures and their microstructures and mechanical properties were investigated.

Experimental Procedures

Materials

Alumina (MR70, Martinswerk Co, mean particles diameter: 0.5-0.8 μm) and WC (Art No.12070, Alfa Aesar Co.) powder were used as the starting materials. The WC powder was mixed with the alumina powder to produce Al_2O_3-WC (0-20 wt %) mixtures. The powders were mixed by ball milling for 12 hrs at 200 rpm with at the presence of small amount of ethanol in a plastic pot. The mixed powders were dried and then passed through a sieve with a pore-opening size of 100 μm. The obtained powders were used to fill a graphite die with an inner diameter of 50 mm and then the powders were sintered using SPS (SPS-20T-10, Easy fashion metal products trade Co.) at temperatures between 1600-1700 °C for a holding time of 600 s at a heating rate of 1 °C/s under vacuum. A uniaxial pressure of 30 MPa was applied and a height of 5 mm was obtained for each of the green samples. The die surface

temperature was measured by an optical pyrometer.

Characterization

Using distilled water, ASTM C373-88 standard via Archimedes method was applied in order to study density changes. The mean density values were obtained by averaging values of densities of three specimens for each composition. The theoretical densities of Al_2O_3 (3.95 g/cm^3), and WC (15.63 g/cm3) were used to calculate relative densities.

The microstructure evolution of the sintered samples was investigated by a field emission scanning electron microscopy (FE-SEM, Mira 3-XMU operating at 30 kV). Siemens diffractometer with Cu Kα radiation (λ = 1.5405 Å) was used to study the phase evolution and crystallinity of the sintered samples. The samples were exposed continuously to Cu Kα radiation (λ = 1.5405 Å) operated at 30 kV/20 mA and at a scanning speed of 1 °/min for a scanning range of 20-80 ° with intervals of 0.02 °.

The test specimens with dimensions of 20 mm × 4 mm× 2 mm were cut and machined for bending strength tests. The entire specimen surface was ground with an 800-grit diamond wheel and the tensile surface was polished by diamond slurries. Bending strength of the samples was measured at room temperature by a three-point bending test operating with a crosshead speed of 0.5 mm/min.

The fracture surfaces were observed using a Mira 3-XMU scanning electron microscope. Following the ASTM-C1327-08 standard the Vickers hardness was measured using a microhardness tester (MVK-H21, Akashi Co.) with a load of 1 kg for 15 sec. The samples surface for the hardness test was prepared through polishing with 1 μm diamond slurry. The average value of 5 measurements for each sample was used to evaluate the Vickers hardness. Anstismethodology [20] was adopted for calculation of the fracture toughness. According to this method, the fracture toughness of the samples was estimated using the following equation:

$$K_{IC} = \varepsilon \left[\frac{E}{H}\right]^{1/2} \cdot \frac{p}{c^{3/2}} \quad (1)$$

Where E is the Young's modulus, H is the hardness, P is the indentation load and 2c is the total crack length (that is, 2c = 2L + 2a, where L is the length of the crack from the indentation corner, and 2a is the indentation diagonal). The term ε is a material constant containing elements related to the geometry of the indenter and the morphology of the crack system.

For each set of mixtures, at least five specimens were tested for measurement of the strength, hardness and fracture toughness.

Results and Discussion

Fig. 1 depicts X-ray diffraction patterns of the alumina reinforced by 5 wt.%, 10 wt.% and 20 wt.% WC sintered at 1700 °C for 600s by SPS. The pattern shows that alumina and the tungsten carbides phases are the only crystalline phases in the samples. This findings is similar to the results reported in the literature for Al_2O_3-WC [5], Al_2O_3 (W,Ti)C [21] and Al_2O_3-TiC [1]. However, this is not the case, for the Al_2O_3-WC-Co composite material produced by vacuum hot pressing as this material exhibits a new crystalline intermetallic phase (Co_3W_3C), which is responsible for the higher hardness values reported in their work [22].

Table 1 shows the relative densities and mechanical properties of various Al_2O_3-WC samples that were analyzed after interrupted sintering at temperatures varying from 1600 °C to 1700 °C with intervals of 50 °C. Considering Fig. 2 and Table 1 one can realize the sintering behavior of the Al_2O_3-5 wt.% WC, Al_2O_3-10 wt.% WC and Al_2O_3-20 wt.% WC powders, respectively. Despite the detrimental effect of the presence of WC phase on sintering, all of the samples have reached over 95% of their theoretical density

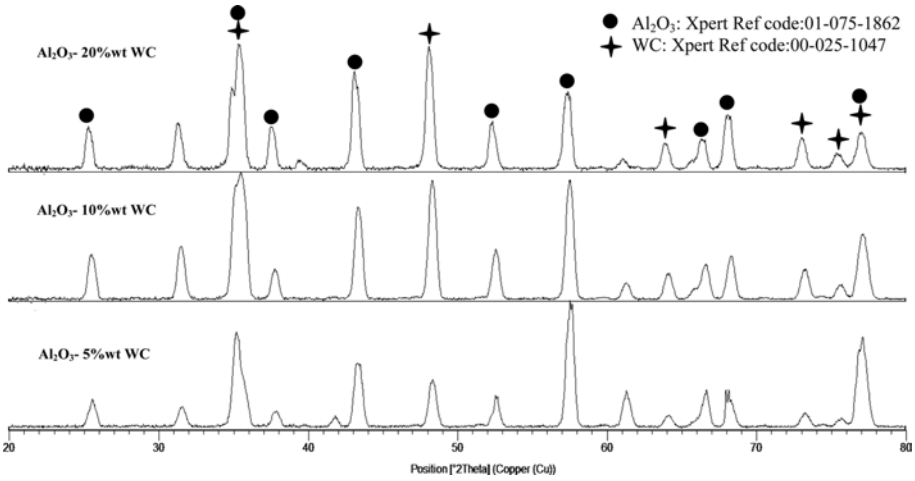

Fig. 1. XRD pattern of alumina-(5 wt.%) WC, alumina-(10 wt.%)WC and alumina-(20 wt.%)WC sintered at 1700 °C for 600s.

Table 1. Relative densities and mechanical properties of various alumina-WC samples that were analyzed after interrupted sintering at temperatures varying from 1600 ºC to 1700 ºC with steps of 50 ºC.

Composition	Temperature (°C)	Relative density (%)	Bending Strength (MPa)	Hardness (HV)
Al_2O_3-(5 wt.%) WC	1600	95.35	317	2011
	1650	97.23	320	2032
	1700	99.07	417	2188
Al_2O_3-(10 wt.%) WC	1600	96	320	2018
	1650	97.41	332	2033
	1700	99.30	463	2208
Al_2O_3-(20 wt.%) WC	1600	93	263	2002
	1650	95.62	312	2010
	1700	98.70	360	2167

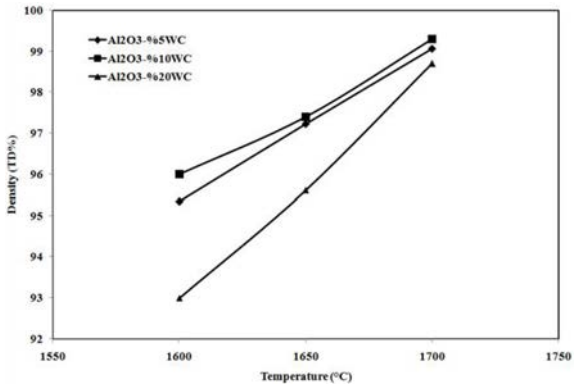

Fig. 2. Sintering curves of Alumina-WC composite powder.

(TD) at 1650 ºC and full densities almost were achieved at 1700 ºC. The contact points between the particles offer high resistance to the current flow and contribute for increased heating. The temperatures at those localized heating zones would exceed the melting temperature of the material and the cumulative effect from all such zones results in increased densification at comparatively lower sintering temperatures and shorter duration than conventional sintering techniques [19].

Fig. 3 shows SEM micrographs of the fractured surface of the samples containing 5 wt% and 10 wt% WC, sintered at 1600-1700 ºC for 600s. Due to the low sintering temperature, the short sintering time and the pining effect of the WC particle on alumina grain growth, a fine matrix grain size is observed for the Al_2O_3-5 wt.% WC and Al_2O_3-10 wt.% WC samples sintered at 1600 ºC. However, when sintering temperature is increased to 1700 ºC, alumina grains become much coarser and less uniform in size. Fracture mode can be explained by an intergranular fracture accompanied by a partial transgranular fracture. The microstructure is homogeneous and the carbide particles are present inside the alumina grains and at grain boundaries. As Fig. 3(c) shows, WC is well uniformly distributed in the alumina matrix. Fig. 3(d) shows that microstructure of the Al_2O_3-(10 wt.%) WC composites sintered at 1700 ºC is dense and contains less visible pores in comparison to other composite

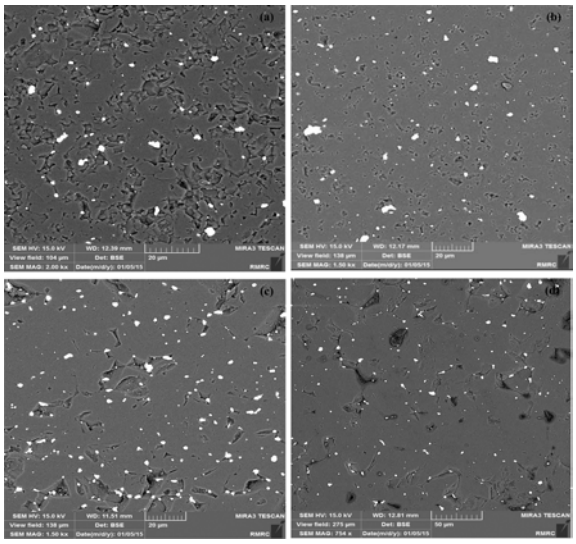

Fig. 3. SEM micrographs of Alumina-WC composites: (a) Alumina-(5 wt.%) WC sintered at 1600 ºC; (b) Alumina-(5 wt.%) WC sintered at 1700 ºC; (c) Alumina-(10 wt.%) WC sintered at 1600 ºC; (d) Alumina-(10 wt.%) WC sintered at 1700 ºC.

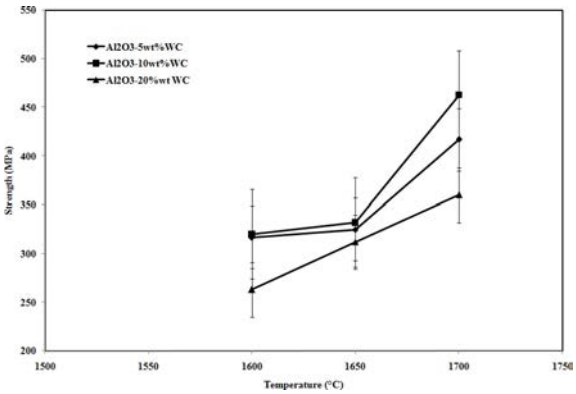

Fig. 4. Plots of effect temperature on the strength of Alumina-WC composite.

combinations.

Fig. 4 shows effect of the temperature on the strength of the Al_2O_3-WC composites. The strength increases steadily by increasing the sintering temperature. At 1700 ºC, the strength of Al_2O_3-5 wt.% WC, Al_2O_3-10 wt.% WC, and alumina-20 wt.% WC composite reach 417 MPa, 463 MPa and 360 MPa, respectively. In comparison with the poor strength of the monolithic alumina sintered by uniaxially hot pressed sintering method (≈280 MPa) [23], the strengths of the present Al_2O_3-10 wt.% WC composites are significantly higher. The increase in Young's modulus, the refined microstructure and the residual stress strengthening effects caused by the presence of WC particle are the most important factors affecting the strength improvement [12].

Fig. 5 shows Vickers hardness of the Al_2O_3-WC composite originally containing 5-20 wt% WC sintered at 1600-1700 ºC for 600s. The Al_2O_3-10 wt.% WC composite sintered at 1700 ºC had the highest Vickers hardness value of 2208 HV. The high hardness of WC

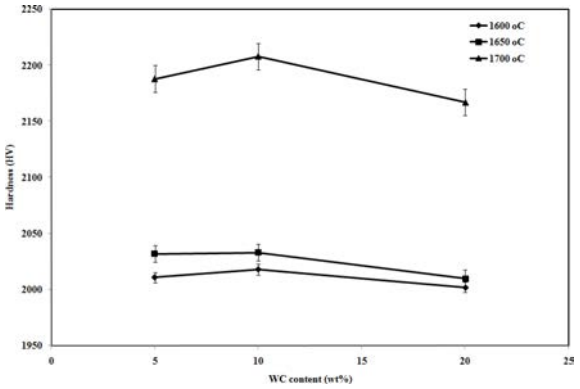

Fig. 5. Effect of WC content on the Vickers hardness of Alumina-WC composite sintered at 1600-1700 °C for 600s.

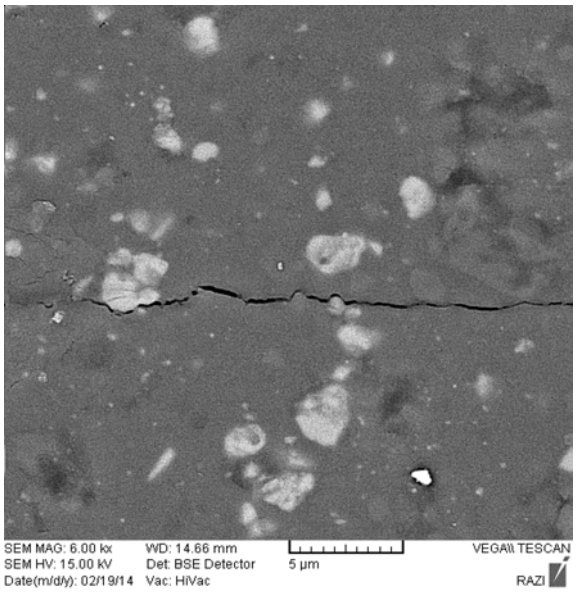

Fig. 6. The SEM image of crack path in Alumina-(10 wt.%) WC composite sintered at 1700 °C by SPS.

particles dispersed in the alumina matrix causes an increase in the hardness. Hardness values for the composite materials ranged between 20 and 22 GPa, are significantly improved compared to that of pure alumina (18.5 GPa). The hardness obtained alumina reinforced with tungsten carbide in the present study was also comparable with values reported in the literature for alumina-TiC [1], (W,Ti)C [24] and WC [6] composites. The hardness of the Al_2O_3-WC composite sintered at 1700 °C decreased with increasing the WC content. Fig. 2 shows that a lower density of the Al_2O_3-WC composite might be the reason for the decrease in the hardness.

Fracture toughness can be determined based on the radial cracks formed at the corners of the indented locations by considering it as a strength limiting flaws in ceramics [25, 26]. With indentation method, the fracture toughness value measured for Al_2O_3-10 wt.% WC sintered at 1700 °C for 600s is 4.15 MPa.$m^{1/2}$. The toughness for Al_2O_3-10 wt.% WC samples that are processed at 1700 °C for 5 min with 30 MPa is significantly higher than the values reported for alumina sintered by SPS at 1150 °C for 3 min with 63 MPa (3.30 MPa $m^{1/2}$) [27]. Also, It is little more to the values reported for the composites Al_2O_3/ 10 vol% SiC and Al_2O_3/10 vol% diamond (2.80 and 3.49 MPa $m^{1/2}$, respectively) [27].

Alumina typically has a fracture toughness of 2.5-3.0 MPa $m^{1/2}$ [28]. This increase in fracture toughness compared to pure alumina can be explained based on the crack propagation behavior. As Fig. 6 shows for the Al_2O_3-WC composite sample, the crack propagation occurred in a zigzag pattern due to crack tip deflection at the WC particles. Further increase in WC particles content hinders crack formation at the corners of the indent mark.

Conclusions

The spark plasma sintering of alumina-WC powder was investigated. The sinterability of the composites increased as the sintering temperature increased. Because of the suppressed grain coarsening and the enhanced mass transport by electric discharge, highly densified Al_2O_3-WC composites were produced at 1650-1700 °C by SPS. The Al_2O_3-WC composite with WC content of 5-20 wt% have reached over 95% of TD at 1650 °C and nearly full density at 1700 °C. The strength and Vickers hardness of Al_2O_3-(10 wt.%)WC composite sintered at 1700 °C had a maximum value of 463 MPa and 2208 HV, respectively. Using the indentation method, a fracture toughness value of 4.15 MPa.$m^{1/2}$ was measured for the Al_2O_3-10 wt.% WC sample.

References

1. R.X. Shi, Y.S. Yin and H. Ge, Materials Science Engineering A 528 (2011) 5341-5347.
2. W. Acchar, C. Zollfarnk and P. Greil, Journal Materials Science 41 (2006) 3299-3302.
3. X.H. Zhang, C.X. Liu, M.S. Li, J.H. Zhang and J.L. Sun, Ceramic International 35 (2009) 93-97.
4. J.K. Daguano, C. Santos, R.C. Souza, R.M. Balestra, K. Strecker and C.N. Elias, International Journal Refractory Metals & Hard Materials 25 (2007) 374-379.
5. D. Jianxin, D. Zeliang, Z. Jun, L. Jianfeng, C.Tongkun, Ceramic International 32 (2006) 499-507.
6. G. Brandt, Materials Technology 14 (1999) 17-24.
7. M.N. Rahaman, L.C. De Jonghe, Proceedings of First International Conference on Ceramic Powder Processing, Orlando FL. 1-4 November 1987.
8. G.W. Scherer, Journal of the American Ceramic Society 70[10] (1987) 719-725.
9. [9] M.W. Weiser, L.C. De Jonghe, Journal of the American Ceramic Society, 71(3) (1988) C125-C127.
10. K. Haberko, Z. Pêdzich, J. Piekarczyk, M.M. Buæko, W. Suchanek, Proceedings of Third Euro-Ceramics, vol. 1, Processing of Ceramics, Eds. P. Duran, J.F. Fernandez., Faenza Editrice Iberica S. L., Hiszpania, (1993) 967-972.
11. C. Zhao, J. Vleugels, B. Basu, O. Van Der Biest, Scripta

Materialia 43 (2000) 1015-1020.
12. D. Ghahremani, T.Ebadzadeh, A.Maghsodipour, Ceramics International 41[2] (2015) 1957-1962.
13. Z. Shen, Z. Zhao, H. Peng, M. Nygren, Nature 417 (2002) 266-269.
14. Z.A. Munir, U. Anselmi-Tamburini, M. Ohyanagi, Journal of Materials Science 41 (2006) 763-777.
15. D.M. Hulbert, D. Jiang, D.V. Dudina, A.K. Mukherjee, Journal of Refractory Metals and Hard Materials 27 (2009) 367-375.
16. B. Klotz, K. Cho, R.J. Dowding, R.D. Sisson Jr., Ceramic Engineering and Science Proceedings 22[4] (2001) 27- 34.
17. B.R. Klotz, K.C. Cho, R.J. Dowding, Materials and Manufacturing Processes 19[4] (2004) 631-639.
18. S. Hayun, S. Kalabukhov, V. Ezersky, M.P. Dariel, N. Frage, Ceramics International 36 (2010) 451-457.
19. D. Ghahremani, T.Ebadzadeh, A.Maghsodipour, Ceramics International 41[5] (2015) 6409-6416.
20. G.R. Antis, P. Chantikul, B.R. Lawn, D.B. Marshall, Journal of the American Ceramic Society 64 (1981) 533-538.
21. W. Acchar, P. Greil, A.E. Martinelli, C.A.A. Cairo, A.H.A. Bressiani and J.C. Bressiani, Journal European Ceramic Society 20 (2000) 1765-1769.
22. W.P. Tai, and T. Watanab, Journal American Ceramic Society 81 (1998) 1673-1676.
23. W. Acchar, C.R.F. da Camara, C.A.A. Cairo, M. Filgueir, Materials Research 15[6] (2012) 821-824.
24. J. Zhao, X. Yuan and Y. Zhou, Materials Science Engineering A 527 (2010) 1844-1849.
25. S.M. Weiderhorn, Annual Review of Materials Science 14 (1984) 373-403.
26. B.M. Moshtaghioun, A.L. Ortiz, D. Gómez-García, A. Domínguez-Rodríguez, Journal of the European Ceramic Society 33 (2013) 1395-1401.
27. G.D. Zhan, J. Kuntz, J. Wan, J. Garay, A.K. Mukherjee, Scripta Materialia 47 (2002) 737-741.
28. K.E. Thomson, D. Jiang, W. Yao, R.O. Ritchie, A.K. Mukherjee, Acta Materialia 60 (2012) 622-632.